Zn-doping effect on the *c*-axis charge dynamics of underdoped high-T_c cuprates

Y. Fukuzumi, K. Mizuhashi, and S. Uchida
Department of Superconductivity, University of Tokyo, Yayoi 2-11-16, Bunkyo-ku, Tokyo 113-8656, Japan
(Received 16 April 1999)

The *c*-axis resistivity and infrared spectrum are investigated for Zn-doped $YBa_2Cu_3O_{7-y}$ and $La_{2-x}Sr_xCuO_4$ in the underdoped regime. We find that the normal-state pseudogap in the *c*-axis optical conductivity is robust in the presence of Zn impurities and that the pseudogap and the divergent *c*-axis resistivity persist even when T_c is suppressed near zero by Zn doping. In the superconducting state a rapid decrease in the *c*-axis Josephson plasma frequency is observed, but the plasma edge remains sharp reflecting the robustness of the low-energy gap feature against Zn doping.

I. INTRODUCTION

The unconventional metallic and superconducting state of high-T_c cuprates manifests itself in their underdoped regime, in particular in their *c*-axis charge dynamics. In the normal state the *c*-axis resistivity (ρ_c) is ''semiconducting'' (ρ_c increases with lowering temperature), while the in-plane resistivity (ρ_{ab}) is metallic.[1] This turns out to be associated with the development of a pseudogap in the *c*-axis optical conductivity [$\sigma_c(\omega)$] spectrum below a characteristic temperature T^* well above T_c.[2] As a consequence of the pseudogap which suppresses the hopping of carriers between CuO_2 planes, the CuO_2 planes form a Josephson coupled array in the superconducting (SC) state, giving rise to the appearance of a sharp plasma edge in the *c*-axis reflectivity spectrum well inside the SC gap region.[3] This edge is now identified as a Josephson plasma mode.[4]

The contrasting behavior of ρ_{ab} and ρ_c has been addressed in the context of both Fermi liquid[5] and non-Fermi liquid.[6] For the non-Fermi liquids the *c*-axis conduction is supposed to be nonmetallic in the ground state so that ρ_c diverges as $T\rightarrow 0$, whereas ρ_c of Fermi liquids recovers metallic conduction at sufficiently low temperatures. In real materials the low-temperature regime is cut off at T_c, so that we cannot know the ground-state property, if superconductivity is not suppressed with, for example, an intense magnetic field or impurity doping. The former was employed by Ando and Boebinger[7] using a 60-T pulsed magnetic field for single-layer cuprates, $La_{2-x}Sr_xCuO_4$ (La214) and $Bi_2Sr_2CuO_{6+y}$ (Bi2201) as they have relatively low upper critical fields. They found that ρ_c diverges logarithmically for both systems, although it is difficult to pursue the pseudogap in pulsed fields.

Zn substitution for planar Cu sites radically suppresses T_c with only a few percent substitution sufficient to kill SC completely. Fukuzumi *et al.*[8] has demonstrated for underdoped cuprates that a superconductor-insulator (SI) transition is induced by Zn doping at the critical sheet resistance near $h/4e^2$. When the Zn content *z* exceeds the critical value z_c, both ρ_{ab} and ρ_c diverges as $T\rightarrow 0$. In recent years, aiming to understand these anomalous Zn-doping effects on the microscopic ground, the effects on Zn doping on the spin dynamics have extensively been studied.[9–12] A focus of these studies is on how Zn affects the gap in the spin excitation spectrum (spin gap) of the underdoped cuprates. The spin gap manifests itself as a peak in the temperature dependence of ^{63}Cu spin-lattice relaxation rate (T_1^{-1}) (Ref. 13) and is closely tied to the pseudogap in $\sigma_c(\omega)$ as well as that observed in the angle-resolved photoemission (ARPES).[14] The result on naturally underdoped $YBa_2Cu_4O_8$ (Y124) and oxygen-reduced $YBa_2Cu_3O_{7-y}$ (Y123) show that the peak in T_1^{-1} is radically suppressed with Zn doping suggestive of a collapse of the spin gap.[9]

The Zn-doping effect on the charge transport is quite contrasting. Mizuhashi *et al.* reported that Zn in $YBa_2Cu_3O_{7-y}$ (Y123) increases the elastic scattering of carriers but does not affect the temperature-dependent part of both in-plane resistivity (ρ_{ab}) and *c*-axis resistivity (ρ_c).[15] The *T* dependence of ρ_{ab} for underdoped materials changes at a characteristic temperature $T^*(>T_c)$ which is correlated with the temperature of the onset of a pseudogap in $\sigma_c(\omega)$ as well as the opening of a spin gap.[16] The finding of Mizuhashi *et al.* implies that probably the excitation spectra relevant to the inelastic charge scattering are not altered by the Zn doping.

In this paper, the Zn doping effects on the *c*-axis charge dynamics are investigated for a typical bilayer cuprate system $YBa_2Cu_3O_{7-y}$ (Y123) and a single-layer $La_{2-x}Sr_xCuO_4$ (La214) in the underdoped regime. The advantages of Zn doping as a probe for charge and spin dynamics are (i) it is applicable to any cuprate system, and (ii) feasible to the optical study to pursue the pseudogap as $T_c\rightarrow 0$. We show that Zn does not affect the basic *T* dependence of ρ_c, and that the semiconducting behavior persists down to near $T=0$ when T_c is suppressed. The persistence of the semiconducting ρ_c arises from the fact that the low-energy region of the pseudogap in $\sigma_c(\omega)$ is almost unaffected by Zn doping and continues to deepen with decreasing temperature. This appears to be linked with a rapid low-energy shift of the Josephson plasma edge in the SC state.

Single crystals of $YBa_2(Cu_{1-z}Zn_z)_3O_{7-y}$ and $La_{2-x}Sr_xCu_{1-z}Zn_zO_4$ were grown by the flux method using a Y_2O_3 crucible and by the traveling-solvent-floating-zone (TSFZ) method, respectively. The details in crystal growth and the sample characterization were described in the previous papers.[8,15] The optical spectra were measured at various

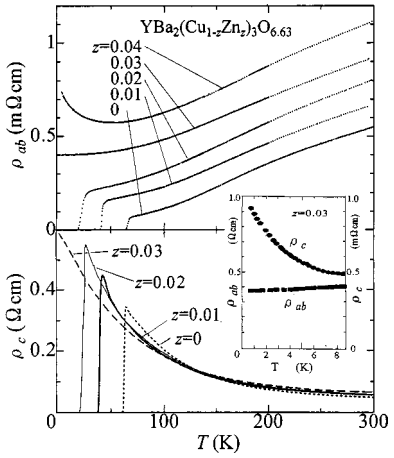

FIG. 1. Temperature dependence of the in-plane (ρ_{ab}) and c-axis resistivity (ρ_c) for Zn-doped $YBa_2Cu_3O_{6.63}$. The inset shows the low-temperature part of ρ_{ab} and ρ_c for the $z=0.03$ crystal located close to the SI transition. The superconductivity observed below 1.3 K is killed by applying a magnetic field (8 T) parallel to the c axis.

temperatures with c-axis polarized infrared radiation in the frequency range above 20 cm^{-1}.

II. EXPERIMENTAL RESULTS

A. Charge transport

The temperature dependences of the in-plane and c-axis resistivity are plotted in Figs. 1 and 2 for a typical 60-K phase $YBa_2Cu_3O_{6.63}$ and $La_{1.85}Sr_{0.15}CuO_4$, respectively, with various Zn contents up to $z=0.04$. Both compounds have nearly the same hole density, and $z=0.03$ is very close to the critical value (z_c) at which an SI transition takes place. In this respect, $x=0.15$-La214 is identified to be in the underdoped regime.[8] For Y123 with $z=0.03$, T_c is suppressed

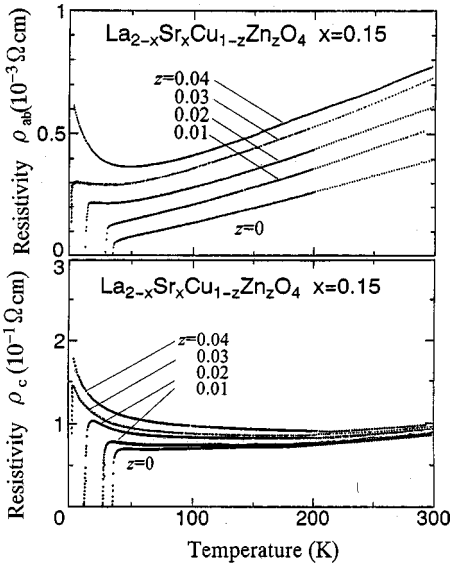

FIG. 2. Temperature dependence of the in-plane and c-axis resistivity for $La_{1.85}Sr_{0.15}Cu_{1-z}Zn_zO_4$ with z up to 0.04.

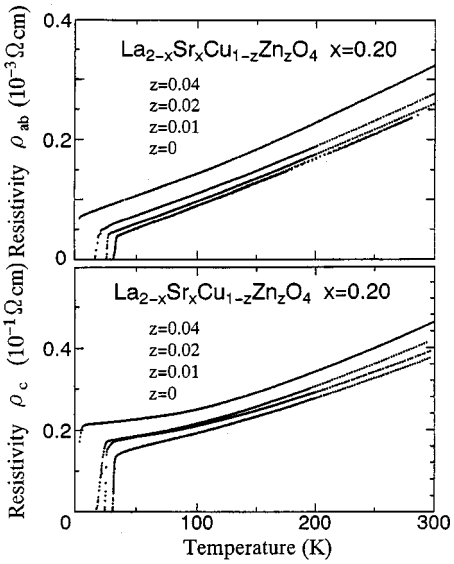

FIG. 3. Resistivities for overdoped material $La_{1.80}Sr_{0.20}Cu_{1-z}Zn_zO_4$ with z up to 0.04 (from bottom to top).

below 2 K and the in-plane resistivity (ρ_{ab}) is metallic down to 2 K, while ρ_c remains semiconducting ($d\rho_c/dT<0$). The semiconducting ρ_c and metallic ρ_{ab} are found to persist down to $T=0.5$ K when minor superconductivity seen in resistivities below 1.3 K is further suppressed by an applied magnetic field of 8 T as shown in the inset. It is evident from Fig. 1 that the effects of Zn doping on ρ_c are very small. At high temperatures Zn only slightly increases the magnitude of ρ_c. At low temperatures the semiconducting T dependence persists, not much affected by Zn doping. As a result, ρ_c increases divergently as T_c is suppressed to near zero at $z\simeq z_c$. The observed $\rho_c(T)$ fits $T^{-\alpha}(\alpha\sim 2)$ down to $\sim$60 K,[1] but shows weaker, either logarithmic or weak power-law ($T^{-\alpha}$ with $\alpha\sim 0.5$) temperature dependence below 60 K.

The contrasting behavior between ρ_{ab} and ρ_c is also seen for the Zn-doped single-layer La214 with $x=0.15$ (Fig. 2). The evolution of ρ_{ab} and ρ_c with Zn doping is basically the same as that for Y123, though the increase in ρ_c with lowering temperature is much weaker, the $\rho_c(T)$ curve shows an up shift with Zn doping. For comparison, we show the result for an overdoped La214 with $x=0.20$ in Fig. 3. For this compound 4%-Zn substitution almost completely destroys superconductivity, but both ρ_{ab} and ρ_c remain metallic. Thus the divergent resistivity only in one direction is characteristic of the underdoped cuprates. This is not a localization phenomenon but an evidence for unconventional charge transport in high-temperature superconductors (HTSC's), pointing toward the charge confinement within the CuO_2 plane.[6]

One may point out an experimental result on the intrisically underdoped Y124 which shows metallic ρ_c at low temperatures.[17] Y124 is perhaps an exceptional system, in which the in-plane charge transport is dominated by the carriers in the double Cu-O chains.[18] The estimated hole density is higher in the chains, which together with much fewer disorder than the chains in Y123, makes the chain conductivity higher than the plane conductivity. Actually, a recent experiment of Y124 has demonstrated that either interchain or chain-plane hopping dominates the c-axis charge transport in this system.[19]

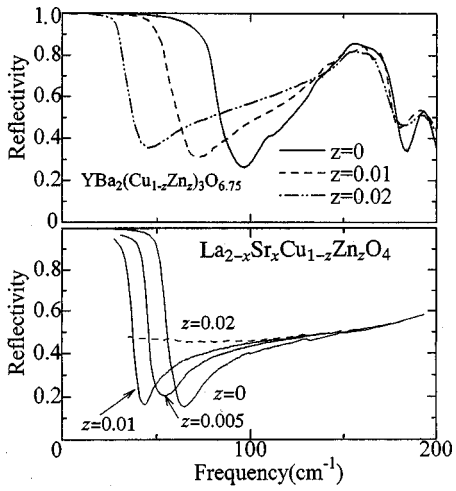

FIG. 4. *c*-axis polarized reflectivity spectra in the superconducting state at $T=10$ K for $YBa_2Cu_3O_{6.75}$ (upper panel) and at $T=8$ K for $La_{1.85}Sr_{0.15}CuO_4$ (lower panel) with various Zn contents.

B. *c*-axis reflectivity spectrum in the superconducting state

In the *c*-axis reflectivity spectrum of the compound $Y123O_{6.63}$, the Josephson plasma edge is seen at ~ 40 cm^{-1} for temperatures well below T_c. The edge rapidly shifts to lower frequency with Zn doping and soon goes out of our frequency limit for *z* exceeding 0.01. In order to experimentally follows the change of the edge frequency with Zn doping, the oxygen content of the crystal has been increased to 6.75 which remains in the underdoped regime and the basic features of the *c*-axis dynamics are not changed. The *c*-axis reflectivity spectra at the lowest temperature are shown in Fig. 4 for $z=0$, 0.01, and 0.02. For $z=0.03$ the edge moves below our experimental limit, but the material goes superconducting ($T_c \sim 15$ K) according to the resistivity and magnetization measurements. The SI transition takes place at $z_c \sim 0.04$ for this oxygen content. Essentially the same change is observed in the *c*-axis reflectivity spectrum of Zn-doped La214 with $x=0.15$. The plasma edge is located at 60 cm^{-1} for Zn-free compound and shifts to 30 cm^{-1} for $z=0.01$, quantitatively the same as in $Y123O_{6.63}$. Note that in both systems the edge remains sharp even for Zn-doped materials.

Reduction of the Josephson plasma frequency (ω_{ps}) with Zn doping is demonstrated in Fig. 5, where unscreened value of ω_{ps} at $T \ll T_c$ is plotted against ρ_c at $T=T_c$ on the logarithmic scales. ω_{ps} is given by the relation $\omega_{ps}^2=\epsilon_\infty \omega_{ps}'^2$, ω_{ps}', and ϵ_∞ being the plasma edge frequency and the dielectric constant above ω_{ps}'. ω_{ps} is related to the *c*-axis London penetration depth λ_c by $\omega_{ps}=1/2\pi\lambda_c$. Also shown in Fig. 5 are the T_c vs ω_{ps} ($\sim 1/\lambda_c$) plots for Zn-free Y123 with various oxygen contents as well as the T_c vs $1/\lambda_{ab}$ (λ_{ab} is the in-plane London length and is inversely proportional to the in-plane plasma frequency of the superconducting carriers) determined by the muon-spin-resonance (μSR) measurement for Zn-doped Y123 with oxygen content of 6.63.[20] The in-plane data follows the well-known universal relationship[21] between T_c and λ_{ab}, $T_c \sim \lambda_{ab}^{-2}$ [shown by the line denoted by (μSR)].

It turns out that both *c*-axis and in-plane data roughly follow the λ^{-1} vs T_c curves for Zn-free compounds. The

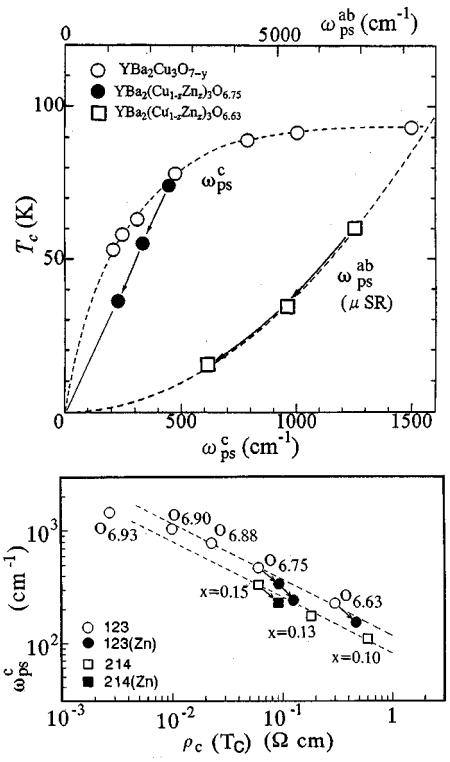

FIG. 5. *c*-axis Josephson plasma frequency plotted against T_c for Zn-free Y123 with various oxygen contents and for Zn-doped crystals with oxygen content of 6.75. Also shown is the in-plane plasma frequency of the superconducting condensate determined by the μSR measurements for Zn-doped $YBa_2Cu_3O_{6.63}$ (Ref. 20). The lower panel illustrates ω_{ps} vs $\rho_c(T_c)$ for various Zn-free and Zn-doped crystals of Y123 and La214.

contrasting behavior between in-plane and *c*-axis property indicates that, while the λ_{ab}^{-1} vs T_c relation is a direct consequence of pair-breaking, i.e., a decrease in the superfluid density n_s with *z*, λ_c^{-1} (or ω_{ps}) vs T_c reflects a decrease in the strength of the Josephson coupling between planes. A linear scaling between ω_{ps}^2 and $\rho_c(T_c)^{-1}$ was found for Zn-free materials with various hole densities.[22,23] As illustrated in the lower panel of Fig. 4, it might be possible to infer that Zn doping decreases ω_{ps} through the increase in the value $\rho_c(T_c)$. The scaling is reminiscent of the Ambegaokar-Baratoff relation for a Josephson-junction array,[24] thus suggesting that ω_{ps}^2 is proportional to the critical current density between planes.

C. *c*-axis pseudogap and superconducting gap

The optical conductivity spectra $\sigma_c(\omega)$ which are obtained via the Kramers-Kronig transformation of the *c*-axis reflectivity data are shown in Fig. 6 for the Zn-doped Y123 $O_{6.63}$ with $z=0$, 0.01, and 0.03. The evolution of $\sigma_c(\omega)$ with Zn doping is basically the same for Y123 with oxygen content 6.75. The normal-state spectrum for the Zn-free crystal shows a pseudogap below $T^* \sim 250$ K. The pseudogap deepens with lowering temperature and continuously transforms into a superconducting gap below $T_c \sim 60$ K. Suppression of conductivity due to the pseudogap and /or the SC gap ex-

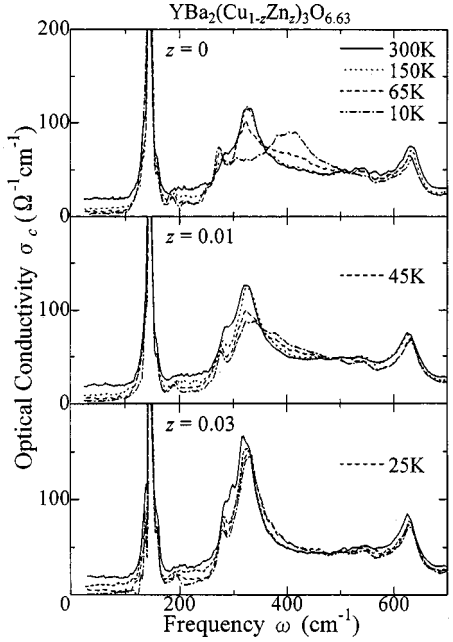

FIG. 6. Kramers-Kronig transformed *c*-axis optical conductivity spectra at various temperatures for Zn-doped $YBa_2Cu_3O_{6.63}$ with $z=0$ ($T_c=60$ K), $z=0.01$ ($T_c=40$ K), and $z=0.03$ ($T_c<2$ K).

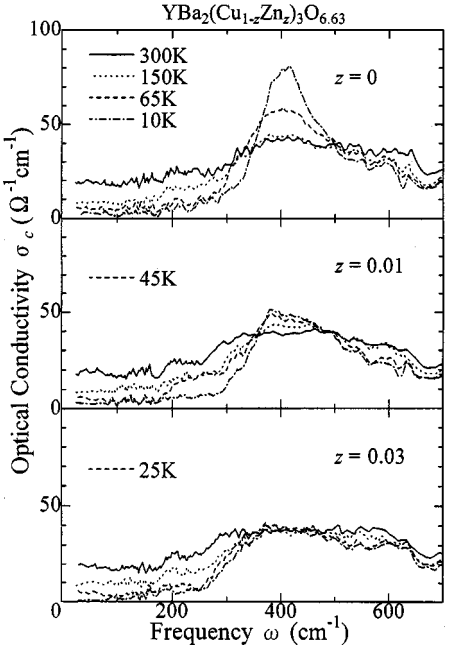

FIG. 7. *c*-axis optical conductivity spectra at $T=10$ K for $YBa_2(Cu_{1-z}Zn_z)_3O_{6.63}$. The phonons are removed from the spectra shown in Fig. 6 except for the broad peak centered around 400 cm^{-1}.

tends to 400–500 cm^{-1} or higher, but the actual gap edge is not clear owing to the dramatic redistribution of the phonon oscillator strengths which takes place below T^* and gives rise to a broad peak centered around 400 cm^{-1}. These features are essentially the same as those previously reported by Homes *et al.*,[2] although the origin of the 400-cm^{-1} peak is not understood yet.

From Figs. 6 and 7 where the spectra with phonons removed (except for the 400-cm^{-1} feature) are shown it is clear that the Zn doping does not change the basic feature of the low-energy spectrum below ~150 cm^{-1} where the spectrum is nearly flat and the conductivity continues to be uniformly suppressed due to the pseudogap and SC gap.

Note that the *c*-axis pseudogap manifests itself even when superconductivity is suppressed. This is consistent with the recent scanning-tunneling spectra of the vortex cores, demonstrating that the normal-state pseudogap goes over continuously into a true SC gap as one moves across the border of the vortex cores.[25]

The robustness the low-energy spectrum against Zn doping is in accord with the result of the dc resistivity shown in Fig. 1 as well as the sharpness of the Josephson plasma edge. The result is in agreement with the work done by Hauff *et al.*,[26] but in contrast to that on Zn-doped Y124 measured by Basov *et al.*[27] The difference between Y123 and Y124 might again be ascribable to the dominant chain contribution in Y124.

The gap structure in $\sigma_c(\omega)$ for Zn-free crystal is somewhat ambiguous at high frequencies due to the appearance of a broad peak centered around 400 cm^{-1}.[2] Zn radically suppresses this anomaly as recently reported by Hauff *et al.*,[26] which makes the high-frequency gap structure legible. The comparison between $z=0.01$ and 0.02 and the spectra with phonons removed (not shown) indicate that the effect of Zn is apparent only at frequencies above ~150 cm^{-1}.

In the case of La214 the pseudogap effect on $\rho_c(T)$ and $\sigma_c(\omega)$ is relatively weak which may be attributed to the single-layer system or to the stronger fluctuation of stripe order in La-based cuprate.[28] However, the opening of a superconducting gap is clearly seen in $\sigma_c(\omega)$ below T_c.[29] Essentially the same Zn doping effect is seen in the SC gap spectrum of La214 as illustrated in Fig. 8. No phonon anomaly is discernible for La214, so we subtract the phonons from the spectra assuming that the phonon contributions do not change across T_c. Actually, as shown in Fig. 8, the conductivity difference between $T=40$ K (just above T_c) and $T=8$ K for $x=0.15$ shows a monotonous variation with ω except for spikelike ''noises'' near the phonon frequencies. In view of the almost flat $\sigma_c(\omega)$ at $T=40$ K,[3] the difference spectrum should display the reduced electronic contribution due to the opening of a superconducting gap. In Fig. 8 are shown the σ_c spectra with phonons removed for Zn-doped ($z=0.01$) La214 with $x=0.15$ at temperature well below T_c. For $x=0.15$ the Zn-free crystal shows a clear SC gap feature, which can roughly fit a model calculation based on the *d*-wave pairing in the CuO_2 planes which weakly and diffusively couple along the *c*-axis.[30,31] Within this model $\sigma_c(\omega)$ is directly connected to the in-plane density of states and shows a knee at ~400 cm^{-1} corresponding to the maximum $2\Delta_0$ of the *d* wave, $\Delta_0(\cos k_x a-\cos k_y a)$, gap. The impurity doping would increase the conductivity over the whole gap region. However, as in the case of the underdoped Y123 most of the Zn-induced spectral weight is located in the high-energy gap region, and the spectrum below ~150 cm^{-1} is not appreciably affected.

The observed Zn-induced change in the SC gap (or pseudogap) spectrum is not anticipated by the theoretical calculations[30,31] based on a Fermi-liquid picture assuming interlayer diffusion model for an impure *d*-wave layered su-

perconductor. This model predicts a uniform increase of the *c*-axis conductivity over the gap region, leading to a decrease in the *c*-axis dc resistivity as a result of impurity-assisted interlayer charge hopping.[5]

III. DISCUSSIONS

A. Zn-doping effect on the *c*-axis gap spectrum

It is worthwhile to compare the present *c*-axis results with the Zn-doping effects on the in-plane charge dynamics.[32,33] In contrast to the *c*-axis dynamics, Zn seriously affects the low-energy in-plane dynamics. In the normal state Zn acts as an elastic potential scatterer in the unitarity limit,[8] giving rise to a large residual resistivity as well as deforming the Drude-like peak in the in-plane optical conductivity spectrum. Basov *et al.*[33] reported that the Drude peak at $\omega=0$ in the pure Y124 crystal changes into a peak positioned at finite frequency in Zn-doped crystals. In the SC state, they showed that Zn produces residual conductivities in the SC gap region of the in-plane optical spectrum, filling in the entire gap down to $\omega\rightarrow 0$. This results in a radical reduction in n_s as observed by μSR,[20,34] which is connected to the rapid suppression of T_c. Therefore the in-plane charge dynamics is influenced by Zn doping over a wide energy range from $\omega=0$ to energy comparable to the width of the *c*-axis pseudogap and/or SC gap.

As mentioned earlier, the measurements of ^{63}Cu T_1^{-1} for Zn doped Y123 and Y124 show that the peak soon disappears upon Zn doping.[9] On the other hand, the neutron inelastic scattering has revealed that the gap persists against Zn doping.[10,11] The ^{63}Cu NMR T_1^{-1} has large contribution from the spin fluctuations near the antiferromagnetic (AF) wave vector (π,π) in the unit of the reciprocal-lattice constant.[35] As the spin gap has the *d*-wave symmetry, the gap node exists for momentum parallel to (π,π), and the gap magnitude is maximum at $(\pi,0)$. The NMR and neutron results suggest that Zn affects the spin fluctuations selectively at momenta near (π,π) (for instance, Zn might widen the gap-node region[36]), while the effect on the spin gap near $(\pi, 0)$ is relatively weak (Zn may slightly decrease the gap magnitude).

In connection with this, the unique Zn-doping effect on the *c*-axis dynamics may result from momentum-dependent interplane hopping. Suppose that the interplane hopping (t_c) has larger contribution from quasiparticles around $(\pi,0)$, as the band-structure calculations yield for bilayer cuprates[37] such that $t_c\sim(\cos k_x a-\cos k_y a)^2$. Also, assuming that Zn has weaker effect on these quasiparticles, then the *c*-axis charge dynamics would sensitively respond to the pseudogap which maximally opens around $(\pi,0)$ and be affected only weakly by Zn doping. Furthermore, owing to dominant contribution to σ_c from near $(\pi,0)$, one may expect a considerably wide flat region in the gapped $\sigma_c(\omega)$ spectrum as well as the robustness of the flat region against Zn doping.

Similar arguments have already been applied to the in-plane dynamics in terms of ''hot spot'' [38] or ''cold spot'' [39] invoking strongly momentum-dependent scattering of electrons. The hot spot is a small region on the Fermi surface near $(\pi,0)$ where the carriers suffur unusually strong scattering, e.g., from the antiferromagnetic spin fluctuations. Because of *d*-wave symmetry the gap, either spin gap or pseudogap arising from pairing fluctuations, most strongly affects the electrons near the hot spot, and hence the contribution to the in-plane resistivity, as experimentally observed by a downturn from linear in T behavior below T^*.[16] Assuming again that Zn has minor effect on the hot spot [or spin fluctuations at $(\pi,0)$], the basic T dependence of ρ_{ab} would not change with Zn doping,[9] consistent with the observation by Mizuhashi *et al.*[15]

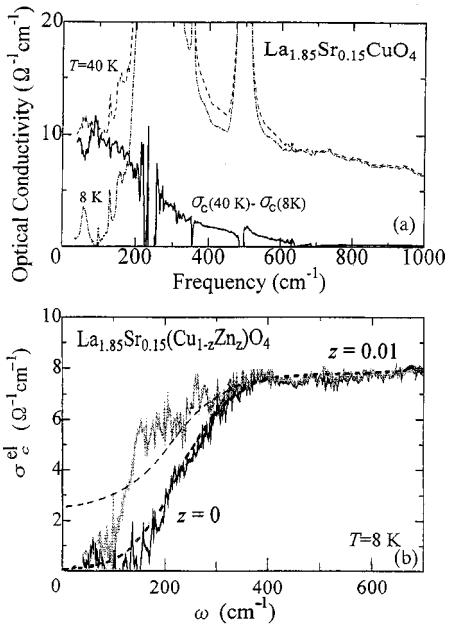

FIG. 8. (a) Difference conductivity spectrum between $\sigma_c(\omega)$ at $T=40$ K (normal state, dashed curve) and $\sigma_c(\omega)$ at $T=8$ K (superconducting state, dot-dashed curve) for $La_{1.85}Sr_{0.15}CuO_4$. (b) Electronic contribution to the *c*-axis conductivity $\sigma_c^{el}(\omega)$ in the superconducting state ($T=8$ K) for $La_{1.85}Sr_{0.15}Cu_{1-z}Zn_zO_4$ with $z=0$ and 0.01. The thick dashed curves are the *d*-wave model calculations after Ref. 30 with $2\Delta_0=370\,\mathrm{cm}^{-1}$ for La214 with $x=0.15$. The impurity effect (in the unitarity limit) on $\sigma_c(\omega)$ expected from the model in Ref. 30 is shown by the thin dashed line in the lower panel.

In relation to the *c*-axis pseudogap, we briefly consider the phonon anomaly which is easily suppressed with Zn doping. The anomaly is observed around 400 cm^{-1} which is incidentally near the maximum $2\Delta_0$ at $(\pi, 0)$ of the *d*-wave anisotropic gap. Thus one may speculate some kind of resonance taking place between optical phonons and electronic gap excitations near $2\Delta_0$. As we have shown, the Zn-doping effect is prominent in the high-frequency gap region, smearing or shifting the structure at $\sim$400 cm^{-1} in $\sigma_c(\omega)$. On the other hand, Hauff *et al.*[26] have suggested a correspondence with the collapse of a peak in the T dependence of NMR T_1 by Zn doping which signals the change of spin fluctuations near (π,π). At present the origin of the 400 cm^{-1} anomaly is not fully understood. The detailed information of the phonon dispersions from neutron experiments is not available for the underdoped Y123.

B. Zn-doping effect on the superconducting condensate

Moving to the superconducting state, the decrease of the plasma frequency ω_{ps}, e.g., at $T=8$ K, appears to be ex-

plained by relating it to the decrease in the missing area of the spectrum between the normal ($T=T_c$) and the SC ($T=8$ K) states as normally done for conventional superconductors,

$$\omega_{ps}^2/8=\int_0^{\omega_c}[\sigma_c^N(\omega,T=T_c)-\sigma_c^S(\omega,T=8\ \text{K})]d\omega, \quad (1)$$

where ω_c is a cutoff frequency, normally $(2\sim4)$ times the gap width, and the superfixes N and S indicate the normal and SC state, respectively. The results in Figs. 6 and 8 indicate that for both Zn-free and Zn-doped materials a major contribution to this integral comes from the missing area below $\sim$150 cm^{-1} due to the opening of a SC gap. $\sigma_c(\omega)$ in this frequency region is nearly flat both at T_c and 8 K due to the pseudogap and SC gap effect, and $\sigma_c(\omega)$ at $T=8$ K is not much influenced by Zn doping. Hence the integral is approximated by the area of a rectangular with the height of $\sigma_c(T=T_c)$ and the width of $\sim$150 cm^{-1}. The value of $\sigma_c(\omega,T=T_c)$ is nearly identical to ρ_c^{-1} in the flat region, so the missing area decreases as $\rho_c^{-1}(T_c)$ increases with Zn content. If one equates it to ω_{ps}^2, then ω_{ps}^2 roughly scales with $\rho_c^{-1}(T_c)$ in qualitative agreement with the experimental result.

However, we have seen in Fig. 1 that for 60 K Y123 $\rho_c^{-1}(T)\sim T^{-0.5}$ at low temperatures. From this the relation $\omega_{ps}^2\sim\rho_c^{-1}(T_c)\sim T_c^{-0.5}$ results which does not reproduce the observed relation $\omega_{ps}\sim T_c$ displayed in Fig. 5. Quantitatively, the rigorous estimate of the missing area is subject to large uncertainty due to the phonon anomaly centered around 400 cm^{-1} in the case of underdoped Y123 and to the presence of gigantic phonon mode at $\sim$250 cm^{-1} in La214.

A rigorous form of the conductivity sum rule should include the integral like Eq. (1), but the normal-sate conductiviy should be $\sigma_c^N(\omega,T=8\ \text{K})$, instead of $\sigma_c^N(\omega,T=T_c)$. Equation (1) is based upon an implicit assumption that the normal state $\sigma_c(\omega,T)$ would be almost identical to $\sigma_c(\omega,T=T_c)$ at any T below T_c. Alternatively, Eq. (1) assumes that the development of the pseudogap suddenly stops at T_c. However, as we have demonstrated here, the normal-state conductivity in the low-ω region continues to decrease when super-conductivity is suppressed by Zn doping, and $\sigma_c^N(\omega,T=8\ \text{K})$ is close to $\sigma_c^S(\omega,T=8\ \text{K})$ below 150 cm^{-1}. Hence the integral in Eq. (1) would be significantly smaller than the c-axis weight of the condensate $(=\omega_{ps}^2/8)$. Anderson argued that, while hopping of single electrons between planes is inhibited due to ''confinement,'' tunneling of pairs is allowed and the formation of pairs results in a gain of kinetic energy which stabilizes the superconducting state and explains the discrepancy between the c-axis spectral weight of the condensate and the missing area in the conductivity.[40] In this interlayer tunneling (ILT) model the c-axis spectral weight of condensate is related to the change in the c-axis kinetic energy between normal and superconducting state, i.e., the condensation energy or Josephson coupling energy E_0,

$$\omega_{ps}^2=4\pi E_0\cdot(2ed), \quad (2)$$

d being the interlayer spacing. E_0 is estimated from the specific heat which is available for Zn doped Y123.[41] Although quantitative test of the ILT model is difficult due to the uncertainties involved in extracting E_0 from the measured specific heat, a decrease in E_0 with Zn doping is obvious. If one assumes the scaling of E_0 to T_c^2, then a linear relation between ω_{ps} and T_c would result, in good agreement with the result for Zn-doped Y123 shown in Fig. 5. As long as the Zn-doping effect is concerned, the ILT model appears to fit better the change of ω_{ps}. However, the empirical relation, reminiscent of Ambegackar-Baratoff, is still applicable to a wide class of high-T_c cuprates and remains to be explained.

IV. SUMMARY

We have investigated the Zn-doping effect on the c-axis charge dynamics of the prototypical high-T_c cuprates in the underdoped regime. It is found that the semiconducting temperature dependence of ρ_c, characteristic of the underdoped cuprates, persists at low temperatures when T_c is suppressed by Zn. This arises from the robustness of pseudogap in the c-axis optical conductivity spectrum in the presence of Zn impurities. Thus the pseudogap is stable even when the superconducting state is inhibited, and can exist without superconductivity. It is anomalous that Zn does nothing to the c-axis charge transport, it neither assists nor disturbs the charges to hop between CuO_2 planes.

Although the result on underdoped Y123 is different from that reported for a related bilayer systems, Y124, it is qualitatively the same as that for a single-layer La214. In view of the not extremely large anisotropy in the present two systems and minor contribution from the chains in Y123, the present results would be generic to the c-axis charge dynamics of HTSC. From these, it can be concluded that the low-energy c-axis charge dynamics is not affected by Zn doping. This, in turn, gives a credit to the insight that the divergent ρ_c as $T\rightarrow0$, while ρ_{ab} remains metallic, is an intrinsic property, evidencing the charge confinement and thus the unconventional electronic state of high-T_c cuprates.

In the superconducting state the predominant effect of Zn doping is to decrease the superfluid density in the CuO_2 plane, which leads to a reduction in T_c. The decrease of the Josephson plasma frequency with Zn doping is indicative of a decrease in the Josephson coupling between planes and appears to be connected with the continuous increase of $\rho_c(T_c)$ as T_c is reduced. The Zn doping effect on the c-axis charge dynamics is in contrast to that on the in-plane charge and spin dynamics in which the effect is weighted toward low-energy region down to $\omega=0$. The result is suggestive of momentum dependent interplane hopping and lifetime of the quasiparticles.

ACKNOWLEDGMENTS

This work was supported by a Grant-in-Aid for Scientific Research and a COE Grant from the Ministry of Education, Science and Culture, Japan, the NEDO Grants for Advanced Industrial Technology Research and for International Joint Research.

[1] S. W. Tozer, A. W. Kleinsasser, T. Penny, D. Kaiser, and F. Holtzberg, Phys. Rev. Lett. **59**, 1768 (1987); D. A. Browner, Z. Z. Wang, and N. P. Ong, Phys. Rev. B **40**, 9329 (1989); L. Forro, C. Ayache, J. Y. Henry, and J. Rossat-Mignot, Phys. Scr. **41**, 365 (1990); T. Ito, H. Takagi, S. Ishibashi, T. Ido, and S. Uchida, Nature (London) **350**, 596 (1991); K. Takenaka, K. Mizuhashi, H. Takagi, and S. Uchida, Phys. Rev. B **50**, 6534 (1994).

[2] C. C. Homes, T. Timusk, R. Liang, D. A. Bonn, and W. N. Hardy, Phys. Rev. Lett. **71**, 1645 (1993); Physica C **254**, 265 (1995).

[3] K. Tamasaku, Y. Nakamura, and S. Uchida, Phys. Rev. Lett. **69**, 1455 (1992); S. Uchida, K. Tamasaku, and S. Tajima, Phys. Rev. B **53**, 14 558 (1996).

[4] M. Tachiki, T. Koyama, and S. Takahashi, Phys. Rev. B **50**, 7065 (1994).

[5] For example, A. G. Rojo and K. Levin, Phys. Rev. B **48**, 16 861 (1993).

[6] For example, P. W. Anderson, Science **256**, 1526 (1992).

[7] Y. Ando, G. S. Boebinger, A. Passner, T. Kimura, and K. Kishio, Phys. Rev. Lett. **75**, 4662 (1995); Y. Ando, G. S. Boebinger, A. Passner, N. L. Wang, C. Geibel, and F. Steglich, *ibid.* **77**, 2065 (1996).

[8] Y. Fukuzumi, K. Mizuhashi, K. Takenaka, and S. Uchida, Phys. Rev. Lett. **76**, 684 (1996).

[9] G.-q. Zheng, Y. Kitaoka, K. Asayama, Y. Kodama, and Y. Yamada, J. Phys. Soc. Jpn. **62**, 2591 (1993); G.-q. Zheng, T. Odaguchi, Y. Kitaoka, K. Asayama, Y. Kodama, K. Mizuhashi, and S. Uchida, Physica C **263**, 367 (1996).

[10] K. Kakurai, S. Shamoto, T. Kiyokura, M. Sato, J. M. Tranquada, and G. Shirane, Phys. Rev. B **48**, 3485 (1993).

[11] Y. Sidis, P. Bourges, B. Hennion, L. P. Regnault, R. Villeneuve, G. Collin, and J. F. Marucco, Phys. Rev. B **53**, 6811 (1996).

[12] K. Ishida, Y. Kitaoka, T. Yoshitomi, N. Ogata, T. Kamino, and K. Asayama, Physica C **179**, 29 (1991).

[13] H. Yasuoka, T. Imai, and T. Shimizu, in *Strong Correlation and Superconductivity*, edited by H. Fukuyama, S. Maekawa, and A. P. Malozemoff (Springer, Berlin, 1989), p. 254.

[14] D. S. Marshall, D. S. Dessau, A. G. Loeser, C.-H. Park, A. Y. Matsuura, J. N. Eckstein, I. Bozovic, P. Fournier, A. Kapitulnik, W. E. Spicer, and Z.-X. Shen, Phys. Rev. Lett. **76**, 4841 (1996); H. Ding, T. Yokoya, J.-C. Campuzano, T. Takahashi, M. Randeria, M. R. Norman, T. Mochiku, K. Kadowaki, and J. Giapintzakis, Nature (London) **382**, 51 (1996).

[15] K. Mizuhashi, K. Takenaka, Y. Fukuzumi, and S. Uchida, Phys. Rev. B **52**, R3884 (1995).

[16] B. Bucher, P. Steiner, J. Karpinski, E. Kaldis, and P. Wachter, Phys. Rev. Lett. **70**, 2012 (1993); T. Ito, K. Takenaka, and S. Uchida, *ibid.* **70**, 3995 (1993).

[17] J.-S. Zhou, J. B. Goodenough, B. Dabrowski, and K. Rogacki, Phys. Rev. Lett. **77**, 4253 (1996).

[18] N. E. Hussey, K. Nozawa, H. Takagi, S. Adachi, and K. Tanabe, Phys. Rev. B **56**, R11 423 (1997).

[19] N. E. Hussey, M. Kibune, H. Nakagawa, N. Miura, Y. Iye, H. Takagi, S. Adachi, and K. Tanabe, Phys. Rev. Lett. **80**, 2909 (1998).

[20] B. Nachumi, A. Keren, K. Kojima, M. Larkin, G. M. Luke, J. Merrin, O. Tchernyshov, Y. J. Uemura, N. Ichikawa, M. Goto, and S. Uchida, Phys. Rev. Lett. **77**, 5421 (1996).

[21] Y. J. Uemura, G. M. Luke, B. J. Sternlieb, J. H. Brewer, J. F. Caralan, W. N. Hardy, R. Kadono, J. R. Kermpton, S. Uchida, H. Takagi, J. Gapalakrishnan, A. W. Sleight, M. A. Subramanian, C. L. Chien, M. Z. Ciepiak, Gang Xiao, V. Y. Lee, B. W. Statt, C. E. Stronach, W. J. Kossler, and X. H. Yu, Phys. Rev. Lett. **62**, 2317 (1989).

[22] T. Shibauchi, H. Kitano, K. Uchinokura, A. Maeda, T. Kimura, and K. Kishio, Phys. Rev. Lett. **72**, 2263 (1994).

[23] D. N. Basov, T. Timusk, B. Dabrowski, and J. D. Jorgensen, Phys. Rev. B **50**, 3511 (1994).

[24] V. Ambegaokar and A. Baratoff, Phys. Rev. Lett. **10**, 486 (1963).

[25] Ch. Renner, B. Revaz, K. Kadowaki, I. Maggio-Aprile, and Ø. Fischer, Phys. Rev. Lett. **80**, 3606 (1998).

[26] R. Hauff, S. Tajima, W.-J. Jang, and A. I. Rykov, Phys. Rev. Lett. **77**, 4620 (1996); S. Tajima, J. Schutzmann, S. Miyamoto, I. Terasaki, Y. Sato, and R. Hauff, Phys. Rev. B **55**, 6051 (1997).

[27] D. N. Basov, R. Liang, B. Dabrowski, D. A. Bonn, W. N. Hardy, and T. Timusk, Phys. Rev. Lett. **77**, 4090 (1996).

[28] J. M. Tranquada, B. J. Sternlieb, J. D. Axe, Y. Nakamura, and S. Uchida, Nature (London) **375**, 561 (1995).

[29] S. Uchida, K. Tamasaku, K. Takenaka, and Y. Fukuzumi, J. Low Temp. Phys. **105**, 723 (1996).

[30] M. J. Graf, M. Palumbo, and D. Rainer, Phys. Rev. B **52**, 10 588 (1995).

[31] P. J. Hirschfeld, S. M. Quinlan, and D. J. Scalapino, Phys. Rev. B **55**, 12 742 (1997).

[32] D. N. Basov, B. Dabrowski, and T. Timusk, Phys. Rev. Lett. **81**, 2132 (1998).

[33] N. L. Wang, S. Tajima, A. I. Rykov, and K. Tomimoto, Phys. Rev. B **57**, R11 081 (1998).

[34] C. Bernhard, J. L. Tallon, C. Bucci, R. De Renzi, G. Guidi, G. V. M. Williams, and Ch. Niedermayer, Phys. Rev. Lett. **77**, 2304 (1996).

[35] M. Mila and T. M. Rice, Phys. Rev. B **40**, 11 382 (1989).

[36] S. Haas, A. V. Balatsky, M. Sigrist, and T. M. Rice, Phys. Rev. B **56**, 5108 (1997).

[37] O. K. Andersen, O. Joseph, A. I. Liechtenstein, and I. I. Mazin, Phys. Rev. B **49**, 4145 (1994).

[38] R. Hlubina and T. M. Rice, Phys. Rev. B **51**, 9253 (1995); B. Stojkovic and D. Pines, Phys. Rev. Lett. **76**, 811 (1996).

[39] L. B. Ioffe and A. J. Millis, Phys. Rev. B **58**, 11 631 (1998); M. Imada, J. Phys. Soc. Jpn. **64**, 2954 (1995), and private communications.

[40] P. W. Anderson, Science **268**, 1154 (1995).

[41] J. W. Loram, K. A. Mirza, J. M. Wade, J. R. Cooper, and W. Y. Liang, Physica C **235–240**, 134 (1994).